COMPILER
Vol. 13, No. 1, May 2024, pp. 55~64
ISSN: 2252-2403 (Print), ISSN: 2549-2403 (Online)
Accredited Fourth Grade by Kemenristekdikti, Decree No:200/M/KPT/2020
DOI: 10.28989/compiler.v13i1.2114

Morphological Study of The Liliba River Utilizing Remote Sensing System

Avilla Martha Anmuni*, Onisius Loden, Jusuf Wilson Meynerd Rafael
Program Studi Teknik Perancangan Irigasi & Penanganan Pantai, Jurusan Teknik Sipil, Politeknik Negeri Kupang.

Article Info

Article history:

Received February 10, 2024
Accepted May 26, 2024
Published May 31, 2024

Keywords:

River Morphology
Liliba
Remote Sensing

ABSTRACT

The branch of natural sciences called river morphology focuses on the study of the characteristics and dynamics of rivers, including their structure, classification, and changes on spatial and temporal scales. Two main factors influence river configurations. The first is natural factors, such as floods and landslides, and the second is human factors, such as human activities that alter river morphology. Cyclone Seroja caused landslides on the banks of the Liliba River in Kupang, East Nusa Tenggara in April 2022. This mainly occurred at Naimata Bridge in Liliba Village, Oebobo District. River geometry, especially the channel and bed elevation, can be significantly influenced by landslides occurring on the riverbanks. Therefore, a study of the morphology of the Liliba River was conducted using remote sensing systems. To conduct a detailed analysis, this study incorporated these photos. In this review, changes in the river channel were examined by extracting the river's course from Landsat image data. From 2009 to 2022, the Liliba River experienced an average shift of 1.60 meters westward and eastward. The research results indicate the need for reforestation along the riverbanks, and residents should be encouraged to reduce the disposal of plastic waste into the river. Future research should also further investigate the geological characteristics of the Liliba River, such as rock types, and conduct hydrological analyses to comprehensively understand the factors influencing changes in the riverbed.

Corresponding Author:

Avilla Martha Anmuni,
Program Studi Teknik Perancangan Irigasi & Penanganan Pantai,
Jurusan Teknik Sipil, Politeknik Negeri Kupang,
Kampus Penfui: Jalan Adisucipto P.O.B.O.X 139 Kupang, 85361.
Email: *avillamartha@gmail.com

1. INTRODUCTION

Rivers are segments on the Earth's surface, including natural reservoirs, channels, and pathways that convey water from the upstream to downstream of a basin and ultimately to the sea (Soewarno, 1995: 20). Rivers possess dynamic characteristics and continually change in response to influencing factors. Generally, changes in rivers encompass alterations in both the quantity and quality of river water and changes in the physical characteristics of the river, with both types of changes mutually affecting each other. Physical changes in rivers can occur in horizontal and vertical geometric parameters.

Natural sciences study the characteristics and behaviour of rivers, their forms, types, and changes. These changes, including spatial and temporal dimensions, are called river morphology. The study of river morphology is divided into three dimensions: 1) Influence of natural phenomena; 2) Movement of water carrying sediments (sediment); and 3) Impact over time.

Human and natural factors are influencing factors in the degradation of river morphology. Natural factors are those caused by nature, such as volcanic eruptions, riverbank landslides, and cold lava floods, while human factors refer to human behaviours in utilizing river embankment areas (Mananoma et al., 2006). For example, continuous human activities can have adverse effects, such as triggering landslides along the riverbanks, which can damage the river flow.

In 2021, Cyclone Seroja struck East Nusa Tenggara, specifically Kupang. The high intensity of rainfall triggered landslides and floods in the rivers of Oebobo Sub-District, in the districts of Oeba, Alam, Fatululi, and Naimata, with water levels reaching 30-60 cm. This information was reported on the Crisis Center website of the Indonesian Ministry of Health on April 5, 2021. Based on observations and interviews with residents living along the Liliba River near Naimata Bridge in Oebobo Sub-District, it was reported that a landslide occurred on the riverbank approximately 80 meters from the bridge, precisely at coordinates 123°37'52.26" E 10°10'27.28" S during the Cyclone Seroja in 2021. After conducting a survey upstream, another landslide was discovered extending for 98 meters from the initial landslide point, precisely at coordinates 123°37'48.56" E 10°10'28.75" S. According to interviews with native residents living along the riverbanks, the landslide was caused by cracks from below and was also influenced by flooding during Cyclone Seroja, resulting in road damage. The damaged road has since been repaired. At coordinates 123°37'49.05" E 10°10'30.68" S, located 57 meters from the second landslide point, damage to residents' land occurred. Landslides - the occurrences of landslides can significantly impact changes in river channels. These alterations in river channels will result in various environmental and social impacts, including navigation issues, flood hazards, and changes in aquatic and riparian ecosystems (Li et al., 2007). Therefore, measuring and observing channel migration from historical aerial photographs is crucial, especially in developing countries, for the development of river system management, flood protection works, and urban planning (Yang *et al*., 1999).[1]

Based on this phenomenon, a research study on the morphology of the Liliba River is conducted utilizing remote sensing systems.

Studying changes in river morphology using remote sensing techniques will aid in monitoring and managing areas, as well as in riverbank protection works.[2] Temporal satellite imagery is utilized for change detection studies (Khan and Jhariya, 2016) with the assistance of GIS tools and models.

Remote sensing and Geographic Information System (GIS) tools extract information and obtain specific measurements regarding spatio-temporal changes in river channels (Aher et al., 2012), providing a comprehensive view of the entire area for monitoring shifts in riverbank lines (Sarkar et al., 2012). The Geographic Information System (GIS)/Remote Sensing technique is now considered a sufficient toolkit for monitoring river behavior and morphology (Resmi et al., 2019; Haq et al., 2012). Remote sensing data is applied to monitor channel shifts, anthropogenic changes, and activities related to land use patterns.[3]

Satellite imagery has been effectively utilized to monitor river processes worldwide in various research projects (Chohan et al., 2015).[4] For monitoring river channel oscillations, remote sensing and GIS are highly efficient and cost-effective, unlike traditional geomorphological investigations, as they provide data integration and a comprehensive overview of the entire coverage area (Langat et al., 2019).

Over the past few years, the unique nature of remote sensing techniques has facilitated the transmission and reception of information over long distances. Organizations such as NASA (National Aeronautics and Space Administration) observe the Earth and other planets through sensors on satellites, recording the reflected or scattered energy. Remote sensors providing broad views and rich data on oceanic systems enable decision-making based on current and future planetary conditions. The development of satellite imagery provides opportunities for accessing information at different times. In addition to comprehensive archives, satellite images must also exhibit maximum spatial and spectral homogeneity to detect changes over time.[5]

2. RESEARCH METHOD

The Liliba River is situated within the Liliba River Basin or Liliba Watershed Area. The Liliba Watershed Area, administratively, is composed of two administrative regions, namely Kupang City and Kupang Province, with a total area of 4,534 hectares and a main river length of 20,176.22 meters.[6]

The research location is situated along the Liliba River, specifically from Naimata Bridge to Liliba Bridge, located in Liliba Village, Oebobo District, Kupang City, covering 2,330.343 meters. The river is divided into three segments. Segment I span 597.283 meters (from 0 to 597.283 meters), while Segment II spans 798.721 meters (from 597.283 to 1396.004 meters), and Segment III spans 934.339 meters (from 1396.004 to 2330.343 meters).

This research employs Landsat image data and Digital Elevation Model (DEM) data. Landsat image data from 10 recording years, namely 2009, 2013, 2015, 2016, 2017, 2018, 2019, 2020, 2021, and 2022, are utilized. The aim is to ascertain the changes during the Liliba River, specifically at Naimata Bridge, before and after the occurrence of Cyclone Seroja. Pre-processing of all Landsat data begins with radiometric correction, involving the conversion of Digital Numbers (DN) values of each band in every image into top-of-atmosphere (TOA) radiance and reflectance values. Subsequently, image quality enhancement procedures are conducted, including image sharpening, spatial filtering, and contrast enhancement. Following this, a combination of the Iso-cluster Unsupervised Classification technique, Principal Component Analysis (PCA), and Natural Difference Water Index (NDWI) is employed to group and accurately delineate the boundaries of

active channels. The results of this combined technique are then converted into polygon format and digitized in ArcGIS to obtain a map depicting the migration of changes in the Liliba River course. Additionally, the merged results of Landsat image data with DEM data are utilized. This combined dataset is then inputted into HEC-RAS using the HEC-GeoRAS plugin in ArcGIS to generate cross-sectional profiles of the Liliba River, facilitating the modeling of changes in its course. Besides using the HEC-GeoRAS plugin, the merged DEM and Landsat image data can also be inputted into HEC-RAS directly, and changes in the riverbed elevation can be modeled using RAS-Mapper.

A. Radiometric Correction

Radiometric correction refers to a series of techniques designed to convert digital values captured by sensors into desired physical quantities, such as light emission, reflection, or surface temperature (Pons and Arcalís, 2012). This transformation is necessary, for example, to facilitate comparisons between remote sensors of the same or different types at different times, as well as to compare satellite or aerial data with data from field-based sensors (Franklin and Giles, 1995). Radiometric correction is also a prerequisite for producing high-quality scientific data (Chander et al., 2009).[7]
Detector irregular response leads to errors in radiometric measurement of digital images. There are cases where regional differences in images do not always directly correlate with differences in quantity and radiation. Image data must be radiometrically calibrated. Drop lines and n-line bands are common errors encountered in satellite images used for Earth observation, such as Landsat or SPOT. Drop lines occur when the scanning machine malfunctions during the scanning process. Mispositioning detectors can result in errors in the lines or bands. Atmospheric refraction and absorption also affect data quality. Atmospheric scattering enhances detail in the image, while atmospheric absorption reduces detail. The use of histograms and regression analysis can help reduce the influence of atmospheric factors that may lead to data errors. Weather stations can be utilized to adjust detectors for better absorption using deformation models.[8]

B. Image Quality Enhancement

Image enhancement is an initial process in image data processing (pre-processing). The objective of image quality enhancement is to obtain images more suitable for further applications (e.g., object recognition within the image). Image quality enhancement is used to improve images that contain noise, are overly bright or dark, lack sharpness, are blurred, suffer from acquisition defects caused by the lens and moving objects during camera movement, and geometric distortions caused by the lens or viewing angle. Image quality enhancement consists of image brightening, image negatives, contrast enhancement, grey-level slicing, and bit-plane slicing.[9]

C. Principal Component Analyses (PCA)

Principal Component Analysis (PCA) is a statistical approach that optimally sorts weighted variables and reduces the dimensions of original data. It has been used in geological problem-solving, such as reservoir channel characterization, geological uncertainty analysis, reservoir modelling, and mineralogy prediction (Jung et al., 2018; Kim et al., 2020; Liu et al., 2020; Yin et al., 2020). PCA has proven successful in reducing information redundancy in previous studies (Ding et al., 2002; Bro and Smilde, 2014). The PCA methodology is employed to reduce the dimensions of feature parameters. To reduce data dimensions, PCA performs a linear transformation to map data from high-dimensional space to low-dimensional space along minimum discrimination directions. PCA exhibits better generalization properties for identifying river network architectures.[10]

D. *Normalized Difference Water Index* (NDWI)

The Normalized Difference Water Index (NDWI) is considered the most suitable index for mapping water bodies. Water bodies exhibit strong absorption and low reflectance in the visible to near-infrared wavelength range. This index utilizes the green and near-infrared bands from remote sensing imagery based on this phenomenon. NDWI can effectively enhance water information in most cases. [11] It is sensitive to built-up land and often results in the overestimation of water bodies. NDWI is calculated as follows using the equation:

$$\mathrm{NDWI} = \frac{(\mathrm{Green}-\mathrm{NIR})}{(\mathrm{Green}+\mathrm{NIR})} \quad (1)$$

Where: Green = Green Band
NIR = Near-Infrared Band

NDWI can also be processed using threshold segmentation methods, target recognition approaches, or other technologies (Li et al., 2018; Jia et al., 2019; Guo et al., 2021).[12]

E. Iso-Cluster Unsupervised Classification

The ISO classification has been employed by Kalantar et al. (2020) in extracting the Zab River channels in Iraq from satellite imagery after georeferencing all images to the UTM coordinate system to identify river evolution.[13] The original Landsat TM images are processed, and color composites are created using various band combinations. Various band combinations provide additional information on objects that can be highlighted with appropriate colors.[14]

F. Segmentation

The optimal segmentation scale for specific applications, which can yield the highest overall classification accuracy with clearly defined polygon feature boundaries and several feature displays with one or more objects. Currently, there are several methods for selecting optimal object-oriented scales, such as the Average Local Variance method and the Maximum Area method, Ratio of Mean Difference to Neighbors to Standard Deviation (RMAS), Standard Deviation of Brightness (SDOM), Mean of Standard Deviations (MOSD), and so forth.[15]

In the classification and extraction of remote sensing imagery, the selection of image resolution and optimal scale directly influences the accuracy of the extracted information. The more precise the chosen scale, the better the image segmentation and the higher the accuracy of the extracted surface features.

Spatial resolution of images has a specific relationship with scale: the higher the spatial resolution, the larger the scale; the lower the spatial resolution, the smaller the scale. It is also observed that higher image resolutions result in better image segmentation effects, while lower image resolutions lead to poorer image segmentation effects.

Perangkat yang digunakan dalam penelitian antara lain:

1. Hardware: Comprising a high-capacity laptop.
2. Sofware:
    a. ArcGIS 10.3
    Through the ArcGIS software, river flow change maps will be obtained. Additionally, it can generate cross-sectional data or river flow using HEC-GeoRAS tools and input the data into HEC-RAS.
    b. Envi 5.3
    Utilized in the process of image data processing starting from radiometric and atmospheric correction, image band merging process, image cropping, image quality enhancement (Image Enhancement), combination of visualization techniques or river cross-section extraction techniques using Principal Component Analyses (PCA), Natural Difference Water Index (NDWI), as well as Iso-Cluster Unsupervised Classification.

The data utilized consists of Landsat satellite imagery from the years 2009, 2013, 2015, 2016, 2017, 2018, 2019, 2020, 2021, and 2022. Landsat data was downloaded from the website https://earthexplorer.usgs.gov/.

Table 1 presents the Landsat Data Employed along with their Extraction or Visualization Techniques.

Year	Satellite Imagery	*Bands Utilized*	Extraction or Visualization Techniques
2009	Landsat 5	3, 4, dan 5	Principal Component Analyses (PCA)
2013	Landsat 8	2 dan 5	NDWI, Isocluster-Unsupervised Classification and PCA
2015	Landsat 8	2, 3, 4, dan 5	Isocluster-Unsupervised Classification
2016	Landsat 8	2 dan 5	Principal Component Analyses (PCA) and NDWI
2017	Landsat 8	2 dan 5	Normalized Difference Water Index (NDWI)
2018	Landsat 8	2 dan 5	NDWI dan Isocluster-Unsupervised Classification
2019	Landsat 8	2, 3, 4, dan 5	Principal Component Analyses (PCA) and

			Isocluster-Unsupervised Classification
2020	Landsat 8	2, 3, 4, dan 5	Principal Component Analyses (PCA) and Isocluster-Unsupervised Classification
2021	Landsat 8	2, 3, 4, dan 5	Principal Component Analyses (PCA) and Isocluster-Unsupervised Classification
2022	Landsat 9	2, 3, 4, dan 5	Principal Component Analyses (PCA)

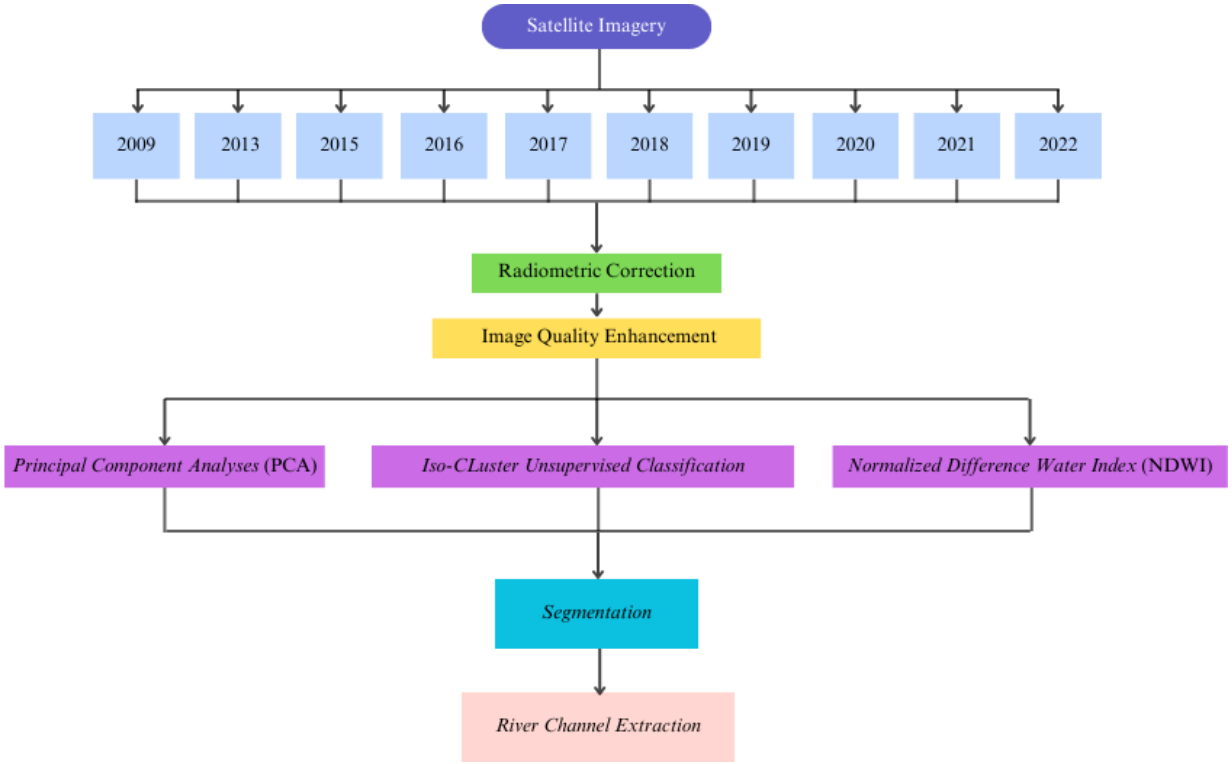

Figure 1 Data Processing Flow

3. RESULTS AND ANALYSIS

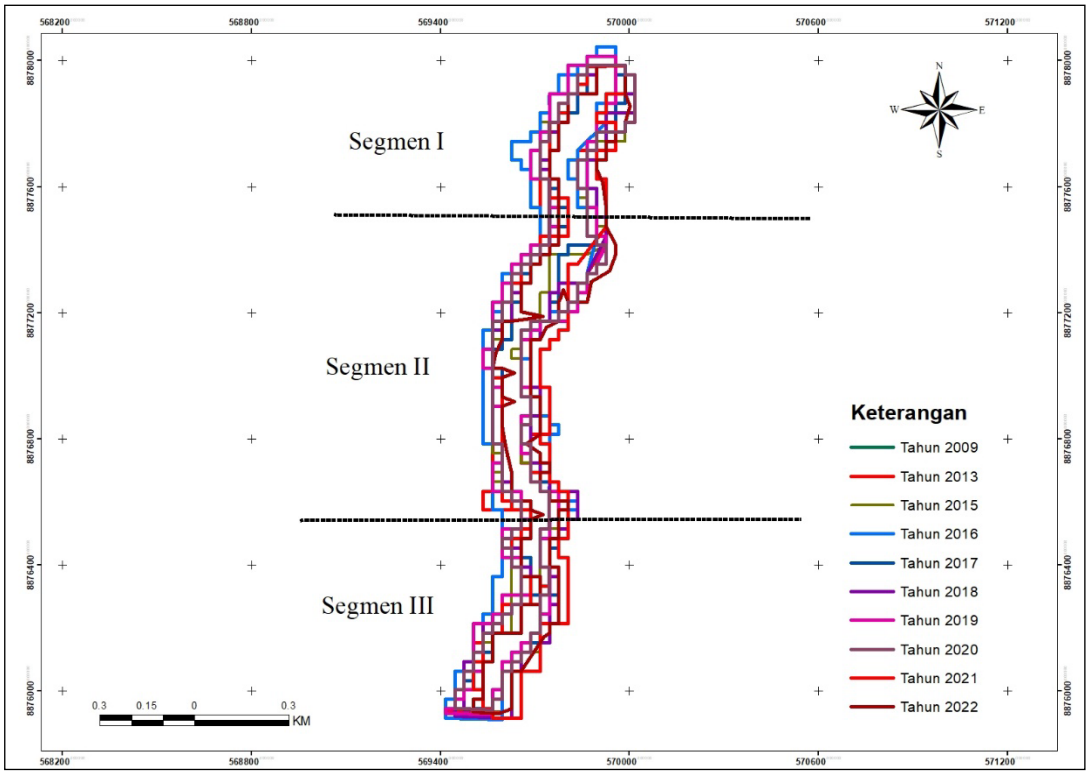

Figure 2 Shift in the Liliba River Channel from 2009 to 2022

Tabel II Shifts in River Channels over the Years 2009, 2013, 2015, 2016, 2017, 2018, 2019, 2020. 2021 and 2022

Year	Segment	Direction		Movement (meter)	Max (meter)	Mean (meter)	Min (meter)
2009 – 2013	I	Left	East	1.3	2.80	1.83	1.20
		Right	West	2.8			
	II	Left	East	1.9			
		Right	West	1.2			
	III	Left	East	2.2			
		Right	West	1.6			
2013 – 2015	I	Left	East	1.63	2.32	1.62	1.23
		Right	West	1.38			
	II	Left	East	1.39			
		Right	West	2.32			
	III	Left	East	1.77			
		Right	West	1.23			
2015 – 2016	I	Left	West	1.83	2.23	1.81	1.46
		Right	West	1.92			
	II	Left	East	1.46			
		Right	West	2.23			
	III	Left	East	1.58			
		Right	West	1.85			
2016 – 2017	I	Left	East	2.81	2.81	2.39	2.10
		Right	East	2.27			
	II	Left	East	2.30			
		Right	West	2.53			
	III	Left	East	2.33			
		Right	East	2.10			

2017 – 2018	I	Left	East	1.14	1.57	1.26	1.13
		Right	East	1.17			
	II	Left	East	1.13			
		Right	East	1.57			
	III	Left	West	1.13			
		Right	East	1.41			
2018 – 2019	I	Left	West	1.41	1.41	1.32	1.20
		Right	East	1.33			
	II	Left	West	1.20			
		Right	East	1.36			
	III	Left	West	1.26			
		Right	west	1.37			
2019 – 2020	I	Left	East	1.20	1.83	1.38	1.09
		Right	East	1.83			
	II	Left	East	1.09			
		Right	West	1.42			
	III	Left	East	1.33			
		Right	East	1.38			
2020 – 2021	I	Left	East	1.25	2.26	1.71	1.21
		Right	West	2.13			
	II	Left	East	1.21			
		Right	West	2.26			
	III	Left	East	1.25			
		Right	West	2.19			
2021 – 2022	I	Left	East	1.11	2.00	1.39	1.11
		Right	West	1.67			
	II	Left	East	1.20			
		Right	West	2.00			
	III	Left	East	1.18			
		Right	West	1.18			
					2.81	**1.60**	**1.09**

From 2009 to 2013, the shift in the river channel on the left side of the river in segment I moved by 1.3 meters to the east. On the right side of the river in segment I, the average shift in the river channel was 2.8 meters to the west. Meanwhile, the river shift in segment II from left to east was 1.9 meters and the river shift from right to west was 1.2 meters. The river channel shift in segment III on the left side of the river averaged 2.2 meters to the east. On the right side of the river, it was 1.6 meters to the west. The largest shift occurred in segment I of the river on the right side, which was 2.8 meters to the west.

From 2013 to 2015, the shift in the river channel on the left side of the river in segment I moved by 1.63 meters to the east. On the right side of the river in segment I, the average shift in the river channel was 1.38 meters to the west. Meanwhile, the river shift in segment II from left to east was 1.39 meters and the river shift from right to west was 2.32 meters. The river channel shift in segment III on the left side of the river averaged 1.77 meters to the east. On the right side of the river, it was 1.23 meters to the west. The largest shift occurred in segment II of the river on the right side, which was 2.32 meters to the west.

From 2015 to 2016, the shift in the river channel on the left side of the river in segment I moved by 1.83 meters to the west. On the right side of the river in segment I, the average shift in the river channel was 1.92 meters to the west. Meanwhile, the river shift in segment II from left to east was 1.46 meters and the river shift from right to west was 2.32 meters. The river channel shift in segment III on the left side of the river averaged 1.58 meters to the east. On the right side of the river, it was 1.85 meters to the west. The largest shift occurred in segment II of the river on the right side, which was 2.23 meters to the west.

From 2016 to 2017, the shift in the river channel on the left side of the river in segment I moved by 2.81 meters to the east. On the right side of the river in segment I, the average shift in the river channel was 2.27 meters to the east. Meanwhile, the river shift in segment II from left to east was 2.30 meters and the river shift from right to west was 2.53 meters. The river channel shift in segment III on the left side of the river averaged 1.85 meters to the east. On the right side of the river, it was 2.10 meters to the west. The largest shift occurred in segment II of the river on the left side, which was 2.81 meters to the east.

From 2017 to 2018, the shift in the river channel on the left side of the river in segment I moved by 1.14 meters to the west. On the right side of the river in segment I, the average shift in the river channel was 1.17 meters to the east. Meanwhile, the river shift in segment II from left to west was 1.13 meters and the river shift from right to east was 1.57 meters. The river channel shift in segment III on the left side of the

river averaged 1.13 meters to the west. On the right side of the river, it was 1.41 meters to the east. The largest shift occurred in segment II of the river on the right side, which was 1.57 meters to the east.

From 2018 to 2019, the shift in the river channel on the left side of the river in segment I moved by 1.41 meters to the west. On the right side of the river in segment I, the average shift in the river channel was 1.33 meters to the east. Meanwhile, the river shift in segment II from left to west was 1.20 meters and the river shift from right to east was 1.36 meters. The river channel shift in segment III on the left side of the river averaged 1.26 meters to the west. On the right side of the river, it was 1.37 meters to the west. The largest shift occurred in segment I of the river on the left side, which was 1.41 meters to the west.

From 2019 to 2020, the shift in the river channel on the left side of the river in segment I moved by 1.20 meters to the east. On the right side of the river in segment I, the average shift in the river channel was 1.83 meters to the east. Meanwhile, the river shift in segment II from left to east was 1.09 meters and the river shift from right to west was 1.42 meters. The river channel shift in segment III on the left side of the river averaged 1.33 meters to the east. On the right side of the river, it was 1.38 meters to the east. The largest shift occurred in segment I of the river on the right side, which was 1.83 meters to the east.

From 2020 to 2021, the shift in the river channel on the left side of the river in segment I moved by 1.25 meters to the east. On the right side of the river in segment I, the average shift in the river channel was 2.13 meters to the west. Meanwhile, the river shift in segment II from left to east was 1.21 meters and the river shift from right to west was 2.26 meters. The river channel shift in segment III on the left side of the river averaged 1.25 meters to the east. On the right side of the river, it was 2.19 meters to the west. The largest shift occurred in segment I of the river on the right side, which was 2.26 meters to the west.

From 2021 to 2022, the shift in the river channel on the left side of the river in segment I moved by 1.11 meters to the east. On the right side of the river in segment I, the average shift in the river channel was 1.67 meters to the west. Meanwhile, the river shift in segment II from left to east was 1.20 meters and the river shift from right to west was 2.00 meters. The river channel shift in segment III on the left side of the river averaged 1.18 meters to the east. On the right side of the river, it was 1.18 meters to the west. The largest shift occurred in segment II of the river on the right side, which was 2.00 meters to the west.

Based on the river channel shift table over the past 10 years from 2009 to 2022, the left side of the river tends to shift towards the east of the river, while the right.

4. CONCLUSION

From the analysis of Landsat image data processing, the following conclusions can be drawn:

1. The change in the Liliba River channel from Naimata Bridge downstream to Liliba Bridge averages 1.60 meters towards both the west and east directions of the river. The most dominant shift occurred from 2016 to 2017 on the left side of segment I of the river, moving 2.81 meters to the east, and from 2009 to 2013 on the right side of segment I of the river, moving 2.80 meters to the west.
2. For small rivers, the Normalized Difference Water Index technique using Landsat satellite imagery Bands 2 and 5 can aid in extracting river channels.
3. The combination of Principal Component Analyses (PCA) and Normalized Difference Water Index (NDWI) techniques can be utilized to extract river channels.
4. Processed image data in raster form can be segmented in ENVI to obtain more accurate vector data.
5. Landsat satellite image processing for the extraction or visualization of small river channels is best performed in ENVI software, which is specialized for satellite image data processing.
6. Further research is needed on the hydrological analysis of the Liliba River using HEC-RAS 6.0 software and a study on the geological characteristics of the Liliba River, such as rock types, using remote sensing systems, as there are many large rocks in the Liliba River.

REFERENCES

[1] S. Baniya, R. Deshar, R. Chauhan, and S. Thakuri, "Assessment of channel migration of Koshi River in Nepal using remote sensing and GIS," *Environ. Challenges*, vol. 11, no. January, 2023, doi: 10.1016/j.envc.2023.100692.

[2] S. Rajakumari, M. Meenambikai, V. Divya, K. J. Sarunjith, and R. Ramesh, "Morphological changes in alluvial and coastal plains of Kandaleru river, Andhra Pradesh using RS and GIS," *Egypt. J. Remote Sens. Sp. Sci.*, vol. 24, no. 3, pp. 1071–1081, 2021, doi: 10.1016/j.ejrs.2021.10.008.

[3] A. R. M. T. Islam, "Assessment of Fluvial Channel Dynamics of Padma River in Northwestern Bangladesh," *Univers. J. Geosci.*, vol. 4, no. 2, pp. 41–49, 2016, doi: 10.13189/ujg.2016.040204.

[4] K. Chohan, S. R. Ahmad, A. Ashraf, M. Kamran, and R. Rasheed, "Remote sensing based innovative solution of river morphology for better flood management," *Int. J. Appl. Earth Obs. Geoinf.*, vol. 111, no. December 2021, p. 102845, 2022, doi: 10.1016/j.jag.2022.102845.

[5] A. Koohizadeh Dehkordi, R. Fatahi Nafchi, H. Samadi-Boroujeni, M. Khastar Boroujeni, and K. Ostad–Ali–Askari, "Assessment of morphological changes of river bank erosion using landsat satellite time-series images," *Ain Shams Eng. J.*, vol. 15, no. 3, p. 102455, 2024, doi: 10.1016/j.asej.2023.102455.

[6] I. N. . Soetedjo, P. De Rozari, and N. Leo, "Studi Penutupan Lahan Hulu dan Hilir Dareah Aliran Sungai Liliba Terhadap Kuantitas Air," *J. Ilmu Lingkung.*, vol. 19, no. 3, pp. 630–637, 2021, doi: 10.14710/jil.19.3.630-637.

[7] X. Pons, L. Pesquer, J. Cristóbal, and O. González-Guerrero, "Automatic and improved radiometric correction of landsat imageryusing reference values from MODIS surface reflectance images," *Int. J. Appl. Earth Obs. Geoinf.*, vol. 33, no. 1, pp. 243–254, 2014, doi: 10.1016/j.jag.2014.06.002.

[8] S. Widjojo, A. Rusmanto, and S. Suharjo, "Pengenalan Proses Citra secara Digital," *Forum Geogr.*, vol. 6, no. 1, p. 55, 2016, doi: 10.23917/forgeo.v6i1.4698.

[9] A. Vyas, S. Yu, and J. Paik, "Image enhancement," *Signals Commun. Technol.*, no. Bagian 1, pp. 199–231, 2018, doi: 10.1007/978-981-10-7272-7_6.

[10] X. Chen, S. Xu, S. Li, H. He, Y. Han, and X. Qu, "Identification of architectural elements based on SVM with PCA: A case study of sandy braided river reservoir in the Lamadian Oilfield, Songliao Basin, NE China," *J. Pet. Sci. Eng.*, vol. 198, no. 66, p. 108247, 2021, doi: 10.1016/j.petrol.2020.108247.

[11] A. K. Taloor, Drinder Singh Manhas, and G. Chandra Kothyari, "Retrieval of land surface temperature, normalized difference moisture index, normalized difference water index of the Ravi basin using Landsat data," *Appl. Comput. Geosci.*, vol. 9, no. December 2020, p. 100051, 2021, doi: 10.1016/j.acags.2020.100051.

[12] Q. S. Du *et al.*, "Extracting water body data based on SDWI and threshold segmentation: A case study in permafrost area surrounding Salt Lake in Hoh Xil, Qinghai-Tibet Plateau, China," *Res. Cold Arid Reg.*, vol. 15, no. 4, pp. 202–209, 2023, doi: 10.1016/j.rcar.2023.08.002.

[13] H. J. Jumaah, M. H. Ameen, G. H. Mohamed, and Q. M. Ajaj, "Monitoring and evaluation Al-Razzaza lake changes in Iraq using GIS and remote sensing technology," *Egypt. J. Remote Sens. Sp. Sci.*, vol. 25, no. 1, pp. 313–321, 2022, doi: 10.1016/j.ejrs.2022.01.013.

[14] P. Lemenkova, "ISO Cluster classifier by ArcGIS for unsupervised classification of the Landsat TM image of Reykjavík," *Bull. Nat. Sci. Res.*, vol. 11, no. 1, pp. 29–37, 2021, doi: 10.5937/bnsr11-30488.

[15] L. Lian and J. Chen, "Research on segmentation scale of multi-resources remote sensing data based on object-oriented," *Procedia Earth Planet. Sci.*, vol. 2, no. 1, pp. 352–357, 2011, doi: 10.1016/j.proeps.2011.09.055.